KDM1A represses the apoptosis in osteosarcoma cells via demethylating Bcl-2/c-Myc

Keywords
endoplasmic reticulum stress, reactive oxygen species, osteosarcoma, demethylation, apoptosis, lysine demethylase 1A, Bcl-2/c-Myc

Abstract

Introduction

Background: Considering the poorly understood mechanism of lysine demethylase 1A (KDM1A) in osteosarcoma (OS), we here commence our investigation to fill the blank.

Material and methods

Methods: Following the transfection as appropriate, 3-[4,5-dimethylthiazol-2-yl]-2,5 diphenyl tetrazolium bromide (MTT) and flow cytometry assays were used to determine the viability and apoptosis of OS cells MG-63, in which the generation of reactive oxygen species (ROS) and the binding between KDM1A and Bcl-2/ cellular Myc (c-Myc) were separately confirmed via DCF-DA method and chromatin immunoprecipitation-PCR. Reverse-transcription quantitative PCR and western blot were finally introduced to quantify the levels of KDM1A/Bcl-2/c-Myc and endoplasmic reticulum (ER) stress-related factors.

Results

Results: Overexpressed KDM1A enhanced the viability (48 hours) yet repressed the apoptosis and ROS generation, with the downregulation on ER stress-related factors (C/EBP homologous protein [CHOP]; proline-rich extensin-like receptor kinase (PERK) and activating transcription factor 4 [ATF4]) yet the elevation of Bcl-2/c-Myc, while its depletion exerted contrary effects. More importantly, KDM1A could act as the demethylase of Bcl-2/c-Myc, as reflected by the results that the depletion of KDM1A decreased the enrichment of Bcl-2/c-Myc promoter using the antibody against KDM1A yet increased the enrichment by the antibody targeting H3K9me2. Bcl-2/c-Myc silencing, conversely, promoted the ROS generation and apoptosis, elevated the levels of ER stress-related factors and abolished the effects of KDM1A on OS cells.

Conclusions

Conclusion: KDM1A exerts a repressive effect on the apoptosis of OS cells MG-63 by inhibiting the ROS generation and ER stress via demethylation of Bcl-2 and c-Myc.

KDM1A represses the apoptosis in osteosarcoma cells via demethylating Bcl-2/c-Myc

Xuezheng Zhao[1], Lijun Li[2], Sihua Zheng[1], Baoyong Tang[1], Yebing Zhang[1], Wei Gao[1*]

[1]*Department of Orthopedics Surgery, Xixi Hospital of Hangzhou, Hangzhou, Zhejiang Province, 310012, China*

[2]*Department of Orthopedics Surgery, The Second Affiliated Hospital, Zhejiang University School of Medicine; Orthopedics Research Institute of Zhejiang University; Key Laboratory of Motor System Disease Research and Precision Therapy of Zhejiang Province, Hangzhou, Zhejiang Province, 310012, China*

* Correspondence to: Wei Gao, Department of Orthopedics Surgery, Xixi Hospital of Hangzhou, No. 2 Hengbu Street, Liuxia town, Xihu District, Hangzhou, Zhejiang Province, 310012, China

Email: gaowei_gwei1@163.com Tel: 86-0571-86481561

Running title: Implication of KDM1A in osteosarcoma

Abstract

Background: Considering the poorly understood mechanism of lysine demethylase 1A (KDM1A) in osteosarcoma (OS), we here commence our investigation to fill the blank.

Methods: Following the transfection as appropriate, 3-[4,5-dimethylthiazol-2-yl]-2,5 diphenyl tetrazolium bromide (MTT) and flow cytometry assays were used to determine the viability and apoptosis of OS cells MG-63, in which the generation of reactive oxygen species (ROS) and the binding between KDM1A and Bcl-2/ cellular Myc (c-Myc) were separately confirmed via DCF-DA method and chromatin immunoprecipitation-PCR. Reverse-transcription quantitative PCR and western blot were finally introduced to quantify the levels of KDM1A/Bcl-2/c-Myc and endoplasmic reticulum (ER) stress-related factors.

Results: Overexpressed KDM1A enhanced the viability (48 hours) yet repressed the apoptosis and ROS generation, with the downregulation on ER stress-related factors (C/EBP homologous protein [CHOP]; proline-rich extensin-like receptor kinase (PERK) and activating transcription factor 4 [ATF4]) yet the elevation of Bcl-2/c-Myc, while its depletion exerted contrary effects. More importantly, KDM1A could act as the demethylase of Bcl-2/c-Myc, as reflected by the results that the depletion of KDM1A decreased the enrichment of Bcl-2/c-Myc promoter using the antibody against KDM1A yet increased the enrichment by the antibody targeting H3K9me2. Bcl-2/c-Myc silencing, conversely, promoted the ROS generation and apoptosis, elevated the levels of ER stress-related factors and abolished the effects of KDM1A on OS cells.

Conclusion: KDM1A exerts a repressive effect on the apoptosis of OS cells MG-63 by inhibiting the ROS generation and ER stress via demethylation of Bcl-2 and c-Myc.

Key words: osteosarcoma, lysine demethylase 1A, apoptosis, reactive oxygen species, endoplasmic reticulum stress, demethylation; Bcl-2/c-Myc

Introduction

As the most prevalent primary malignancy of the bone associated with a high propensity for local invasion and metastasis, osteosarcoma (OS) is a rare tumor for which complex multidisciplinary management is needed [1, 2]. However, due to the diverse histological patterns and the shortage of diagnostic biomarkers for most cases, the diagnosis of OS can be challenging [3]. As such, the identification of the underlying mechanism concerning the evolution of OS will be of help in the better management of this rare malignancy [4].

Recent years have also witnessed the increasing research highlighting the possibility to cluster OS on the basis of identifying candidate driver genes and developing targeted therapy using elaborated sequencing analyses [5]. The genes B-cell lymphoma-2 (Bcl-2) and cellular Myc (abbreviated as c-Myc and known as MYC as well) have been widely reported to participate in the control of cell cycle and/or the programmed cell death, in addition to the suggestion on their impact on the biological behaviors of malignancies, OS, for instance [6, 7]. Specifically, the expression patterns of Bcl-2 and c-Myc and their correlation with the prognosis of patients have been discussed in an existing study [7]. It has been underlined that Bcl-2 posed a regulatory effect on the mitochondrial metabolism for the generation of reactive oxygen species (abbreviated as ROS, the accumulation of which induces the apoptosis of OS cells via mediating the endoplasmic reticulum (ER) stress), while such generation of ROS is indicated to be suppressed by MYC, another prognostic biomarker and therapeutic target of OS [8-11]. Linking the keywords “Bcl-2/c-Myc”, “ROS accumulation”, “ER stress” and “OS” together, we have the reason to believe that Bcl-2/c-Myc may pose regulatory effects on both ROS accumulation and ER

stress in OS and herein commence our research to investigate the possible mechanisms implicated and the potential regulator(s).

Furthermore, the possible efficacy of DNA demethylation therapy in OS has been indicated, with the underlying mechanism vague [12]. Considering the pivotal role of DNA methylation status in the most prevalent molecular alternations during tumorigenesis and the outcome of DNA methylation on the obstruction of the promoter region (which hampers the transcription of gene and leads to gene silencing), it remains a challenge to identify the optimal biomarkers which either regulates or be regulated by DNA methylation/demethylation during the progression of OS [13, 14]. Lysine demethylase 1A (KDM1A), also known as lysine-specific histone demethylase 1 (LSD1), symbolizes the first example of the identified nuclear protein with histone demethylase activity [15]. Specifically, the special role of KDM1A in the epigenetic regulation of gene expression has been discovered and discussed, as reflected by its capability of removing methyl groups from mono- and demethylated lysine 4 and/or lysine 9 on histone H3 (i.e., H3K4me1/2 and H3K9me1/2) and its behaviors as the repressor or activator of gene expression [15, 16]. And previous study showed that cisplatin directly down-regulate KDM1A protein expression in a dose-response manner, suggesting that KDM1A is a downstream target of cisplatin [17]. Indeed, the promoting effects of KDM1A on the occurrence of OS has been proposed, with a proposal with regards to its inhibitory effect on the expression of E-cadherin (CDH-1) by its function as the demethylase [18, 19]. Considering the dearth of research addressing the possible implication of KDM1A/Bcl-2/c-Myc and the role of KDM1A as the demethylase of Bcl-2/c-Myc in OS, we set about to solve this mystery and commence our research, the results of which are reported as

follows.

Material and methods

Cell culture

Human OS cell line MG-63 (TCHu124, Shanghai Cell Bank, Chinese Academy of Science, Shanghai, China) was cultured in minimal essential medium (MEM, E600020, Sangon Biotech, Shanghai, China) blended with 1.5 $g \cdot l^{-1}$ sodium bicarbonate ($NaHCO_3$, A100865, Sangon Biotech, China), 0.11 $g \cdot l^{-1}$ sodium pyruvate ($C_3H_3NaO_3$, A100342, Sangon Biotech, China) and 10% bovine calf serum (BCS, E600001, Sangon Biotech, China) as recommended by the supplier. Heracell™ VIOS 160i CO_2 incubator (51033559, ThermoFisher, Waltham, MA, USA) was used to ensure the growth of cells, with the culture condition adjusted to 37℃ with 5% CO_2.

Transfection

Prior to the transfection, the pcDNA 3.1 vector (V790-20, Invitrogen, Carlsbad, CA, USA) was used to construct the overexpression vector of KDM1A (hereafter represented as “KDM1A” in the figures) via inserting the whole sequence, with the empty vector without insertion as the negative control (hereafter stylized as “NC” in the figures). Meanwhile, the short hairpin RNA against KDM1A (abbreviated as shKDM1A, C02001) and the corresponding negative control (shNC, C03002) were synthesized and obtained from GenePharma (Shanghai, China), where the small interfering RNAs (A01001) against Bcl-2 (siBcl-2) and MYC (siMYC) as well as their negative control (siNC, A06001) were available as well. The sequences used here were provided in Table 1 for reference.

For the transfection, all processes hereafter were strictly repeated based on the

manufacturer's protocols. In a nutshell, MG-63 cells (1×10^6 cells per well in the 6-well plates) were allowed to grow until the confluence of 90% was reached prior to the transfection. The transfection reagent lipofectamine 2000 (11668-030, Invitrogen, USA) and the plasmids were pre-diluted in the Opti-MEM® medium (22600-050, Gibco, Grand Island, NY, USA) in advance, followed by the addition of plasmids into the transfection reagent for the 5-minute incubation at room temperature and the introduction of plasmid-lipid complex to MG-63 cells for the final incubation at 37℃ for 48 hours. All cells were subsequently collected for subsequent analyses.

Cell viability and apoptosis assay

In order to evaluate the viability and apoptosis of MG-63 cells following the different intervention, a commercial 3-[4,5-dimethylthiazol-2-yl]-2,5 diphenyl tetrazolium bromide (MTT) cell proliferation assay kit (E606334) and Annexin V apoptosis detection kit (E606336) were purchased from Sangon Biotech.

For the viability assay, MG-63 cells were maintained in the 96-well plates at the density of 2×10^3 cells per well and incubated for 48 hours, and then the prepared MTT solution (5 mg/ml) in the final volume of 10 microliter (μl) was added into the plates for additional 4-hour incubation. The formazan solubilization solution provided by the kit was added following the careful removal of culture medium in each well, after which a gentle shake was conducted for 10 minutes until the formazan formed was fully dissolved. The absorbance at 570 nm was read with the help of the iMark microplate absorbance reader (1681135, Bio-Rad, Hercules, CA, USA) and the viability of MG-63 cells was calculated as appropriate.

For cell apoptosis assay, the binding buffer was pre-diluted and added into MG-63

cells to suspend the cells to the required density of 2×10^5 cells per milliliter (ml). The working solution of both Annexin V-FITC (5 μl) was then added to the cells for the incubation at room temperature for 15 minutes without light. After the rinse with 200 μl binding buffer and the centrifugation at 100 rpm for 5 minutes, the supernatant was discarded and cells were continued to be resuspended in 190 μl binding buffer and added with 10 μl propidium iodide working solution. CytoFLEX S flow cytometer (C09765, Beckman Coulter, Indianapolis, IN, USA) was used to acquire the data, which were finally processed in the affiliated CytExpert software (Beckman Coulter, USA).

Cellular ROS generation determination assay

DCFDA cellular ROS assay kit (ab113851, Abcam, Cambridge, UK) was employed to assess the generation of ROS in MG-63 cells with different intervention [20]. For the determination, MG-63 cells were allowed to adhere overnight in the 96-well plates with the indicated density of 2.5×10^4 cells per well, following which the medium was removed and cells were dyed using 100 μl/well of the diluted DCFDA working solution at 37℃ for 45 minutes in the dark. The working solution was then replaced with the buffer and the supplement buffer (two separate terms provided with the kit) at the same concentration. The Excitation Wavelength/Emission Wavelength (Ex/Em) at 485/535 nm was read in a fluorescence plate reader (PHERAstar FSX, BMG Labtech, Cary, NC, USA).

Chromatin Immunoprecipitation-PCR (ChIP-PCR) analysis

A ChIP kit (ab500) ordered from Abcam was used and all processes conducted here were based on the protocols of producer and previous research [21]. In detail, MG-63 cells in the 6-cm dish (3×10^6 cells) were transfected with the shKDM1A/shNC for 2

days as appropriate, followed by the harvest and fixation in the formaldehyde (HCHO, A501912, Sangon Biotech, China) for 10 minutes. Then the cell pellets were sonicated, with the removal of residue via the centrifugation. Following the incubation of primary antibodies against IgG (ab172730, Abcam, UK), KDM1A (ab195405, Abcam, UK) and H3K9me2 (PA5-120810, Invitrogen, USA) at 4℃ overnight, cells were continued to be treated with proteinase K (A004220, Sangon Biotech, China) and the DNA was harvested. SYBR Green Fast qPCR mix (K1070, APExBio, Houston, TX, USA) was used to determine the relative enrichment in the promoter of both Bcl-2 and MYC as guided by the manufacturer. The primers used were listed in the section of "reverse-transcription quantitative PCR".

RNA extraction and reverse-transcription quantitative PCR

The total RNA of MG-63 cells with different intervention was extracted using the conventional method with the help of TriZol reagent (15596-026, Invitrogen, USA) and preserved at -80℃ until use. Following the assay to quantify its concentration with the spectrophotometer (ND-2000, ThermoFisher, USA), the cDNA synthesis kit (B300537, Sangon Biotech, China) was employed to synthesize the cDNA. The PCR was finally run using SYBR Green Fast qPCR mix and CFX96 PCR system (1845096, Bio-Rad, USA) at the conditions: 95℃ for 2 minutes, followed by 40 cycles of 95℃ for 15 seconds and 60℃ for 30 seconds, as recommended by the manuals. For the quantification of relative mRNA levels, a calculation method called 2(-Delta Delta C(T)) method was used, with glyceraldehyde-3-phosphate dehydrogenase (GAPDH) as the housekeeping control [22]. The primers used were listed in Table 2.

Western blot

The protein expressions of Bcl-2/MYC and ER stress-related factors in MG-63 cells with the indicated intervention were quantified via western blot as appropriate [23]. In detail, the total protein of MG-63 cells was extracted with the RIPA lysis buffer (C500005, Sangon Biotech, China) and its concentration was evaluated by bicinchoninic acid (BCA) protein assay kit (C503021, Sangon Biotech, China) as appropriate.

For subsequent analyses, the protein sample was detached on SDS-PAGE (C631100, Sangon Biotech, China) and transferred to the PVDF membrane (F619537, Sangon Biotech, China), after which the membrane pre-blocked with 5% defat milk was probed with the primary antibodies (Abcam, UK) against Bcl-2 (ab182858, 26 kDa, 1:2000), MYC (ab32072, 57 kDa, 1:1000), C/EBP homologous protein (CHOP, ab11419, 31 kDa, 1:2000), proline-rich extensin-like receptor kinase (PERK, ab79483, 125 kDa, 1:1000), activating transcription factor 4 (ATF4, ab184909, 50 kDa, 1:1000) and housekeeping control GAPDH (ab226408, 36 kDa, 1:1000) at 4℃ overnight. Furthermore, for the incubation of horseradish peroxide-conjugated secondary antibodies (which was carried out at room temperature for 1 hour), the antibodies of goat anti-rabbit IgG (D110058, Sangon Biotech, China) and goat anti-mouse IgG (D110087, Sangon Biotech, China) were used at the dilution ratio of 1:5000.

For the visualization process, the membrane which has been treated with the ECL luminescence reagent (C510043, Sangon Biotech, China) was exposed to ChemiDoc Touch imaging system (Bio-Rad, USA) and the grey value of the membrane was determined in the affiliated Image Lab™ Touch software as needed.

Data analyses and processing

All data of at least three independent assays were expressed as mean ± standard deviation (SD) and analyzed in Graphpad 8 (Graphpad, Inc., La Jolla, CA, USA). Data between two groups or among multiple groups were compared with independent *t* test and one-way analysis of variance, with Bonferroni *post hoc* test employed as well. The statistical significance was defined when the *p*-value was lower than 0.05.

Results

KDM1A overexpression inhibited ROS generation and apoptosis yet promoted the viability of OS cells MG-63, while its knockdown led to contrary results

In the beginning, we transfected the overexpression plasmid of KDM1A (presented as KDM1A in the figures) and shRNA against KDM1A (stylized as shKDM1A) into OS cells MG-63 to reveal the effects of KDM1A on the malignant behaviors of OS cells, which was proved to be successful, as reflected by the elevated or decreased KDM1A level in MG-63 cells following different transfection (Figure 1A, $p<0.001$). Meanwhile, based on the MTT (Figure 1B) and flow cytometry assay (Figure 1C-D), the knockdown of KDM1A led to a suppressed viability at 48 hour and an increased apoptosis in MG-63 cells (Figure 1B-D, $p<0.001$), while its overexpression did conversely to promote the viability and inhibit the apoptosis (Figure 1B-D, $p<0.01$). Considering the role of ROS production in the induction of apoptosis in OS cells [9], the production of ROS in MG-63 cells with either the knockdown or the overexpression of KDM1A was calculated, where it was evident that the overexpression of KDM1A diminished the ROS production (Figure 1E, $p<0.05$), whereas the knockdown of KDM1A produced different results to aggravate the ROS production (Figure 1E, $p<0.001$). These results thus indicated that

KDM1A may aggravate the malignant behaviors of OS cells.

KDM1A overexpression inhibited the ER stress yet promoted the expressions of Bcl-2/MYC in OS cells MG-63, while its silence did conversely

Likewise, the significant role of ER stress in the apoptosis of OS cells has been emphasized as well [9]. Herein, we measured some related factors, including CHOP, PERK, and ATF4, were quantified in MG-63 cells after the intervention as appropriate, where it became evident that the silence of KDM1A increased the expressions of all these factors (Figure 2A-B, $p<0.001$), whilst KDM1A overexpression produced contrary results (Figure 2A-B, $p<0.001$). Furthermore, with the proposal on the prognostic value of Bcl-2/MYC in OS patients [7], we assumed that Bcl-2/MYC might participate in the mechanism by which KDM1A exerted its effects on OS cells. Accordingly, the levels of Bcl-2/MYC were quantified, where it was observable that the silence of KDM1A inhibited the expressions of Bcl-2/MYC (Figure 2C-F, $p<0.01$), such effects of which were opposite to those following the overexpression of KDM1A (which promoted the levels of Bcl-2/MYC) (Figure 2C-F, $p<0.001$), proving the regulatory effects of KDM1A on the ER stress and Bcl-2/MYC in OS.

KDM1A could demethylate Bcl-2/MYC in OS cells MG-63

The role of KDM1A as the demethylase of CDH-1 in OS has illuminated us to the speculation whether KDM1A could also demethylase Bcl-2/MYC in OS cells as well [19]. Herein, ChIP-PCR analysis was performed as needed, where it was observed that the depletion of KDM1A led to the decreased enrichment of Bcl-2/MYC promoter using the antibody against KDM1A yet caused the increased enrichment by the antibody against H3K9me2, an important epigenetic modifier of several processes (Figure 3A-D,

p<0.01) [24]. It was thus suggested that KDM1A posed negative regulatory effects on Bcl-2/MYC in an H3K9-dependent manner.

The silence of Bcl-2/MYC abolished the effects of KDM1A on the ROS production, ER stress and apoptosis of OS cells

With the hope to investigate the interplay between KDM1A and Bcl-2/MYC, the siRNA against Bcl-2/MYC was transfected into OS cells, where it was found that all these siRNAs decreased the levels of Bcl-2/MYC in OS cells (Figure 3E-F, p<0.01), and those with the most significant knockdown effects (siBcl-2#3 and siMYC#2) were employed for subsequent assays.

When it comes to the ROS production, Bcl-2/MYC silencing led to a sharp increase of ROS production in OS cells MG-63 (Figure 3G-H, p<0.001), whereas the overexpression of KDM1A did oppositely (Figure 3G-H, p<0.05). Furthermore, we found that such effects of overexpressed KDM1A on the ROS production in OS cells were diminished via Bcl-2/MYC silencing (Figure 3G-H, p<0.001).

As to the protein expression of ER stress-related factors, the silence of Bcl-2/MYC aggravated the levels of CHOP, PERK, and ATF4 (Figure 4A-D, p<0.01), the results of which were contrary to those following the overexpression of KDM1A (Figure 4A-D, p<0.01). Likewise, the silence of Bcl-2/MYC also neutralized the effects of KDM1A overexpression on the ER stress-related factors in OS cells (Figure 4A-D, p<0.01).

Finally, based on the data of flow cytometry, KDM1A overexpression led to a suppressive effect on the apoptosis of OS cells MG-63 (Figure 5A-D, p<0.001), while Bcl-2/MYC silencing did oppositely and abolished the suppressive effects of overexpressed KDM1A on the apoptosis of OS cells MG-63 (Figure 5A-D, p<0.05).

Taken together, we concluded that KDM1A exerted its effects on the ROS production and ER stress and OS cells so as to modulate the apoptosis via demethylating Bcl-2/MYC.

Discussion

Existing research has underlined the role of KDM1A as a histone demethylase during the carcinogenesis, showing the emerging option of targeting KDM1A as a therapeutic option for cancers [25]. Indeed, KDM1A has been proposed to have association with different aspects of tumors, the epigenetic regulation of epithelial-to-mesenchymal transition, the stemness and drug resistance, to name a few [26-28]. Furthermore, the promoting effects of KDM1A on the occurrence of OS has been well-reported, and more importantly, it has been stressed that KDMI1A, being a demethylase, unleashed its inhibitory effect on the expression of CDH-1 [18, 19]. Considering these, we have the reason to believe that there must exist other candidate(s) that could both be demethylated by KDM1A and participated in the underlying mechanism with regards to the effects of KDM1A exerted on OS. Upon seeking the candidate(s), Bcl-2 and c-Myc caught our attention in that they have been widely reported to participate in different malignancies, OS, for instance [6, 7]. Further experiments have led us to conclude that KDM1A could indeed demethylate Bcl-2/c-Myc so as to exert its effects on OS, which, to some extent, additionally proved the participation of KDM1A on OS in a way.

Previous investigation has underlined the fact that the excessive apoptosis may result from the ROS and ER stress, and both ROS and mitochondria play critical roles in the induction of apoptosis under the pathologic and physiologic conditions [29, 30]. In other words, when at high levels, ROS may induce oxidative stress, resulting in the oxidative damage in the mitochondria and the onset of certain human pathologies like

tumors, despite the fact that low level of ROS can be beneficial [31-33]. More importantly, what distinguishes the malignant cells from the normal cells is their capability of producing increasing number of ROS and their elevated dependence over the antioxidant defense system [33]. Also, it should be aware that apart from mitochondria, the ER, being regulated by ROS as well, is a crucial regulator of the cell death signaling pathway, with mitochondria being another [34]. Under the prolonged and severe ER stress, the unfolded protein response (UPS), a sequence of reactions underlined to restore the homeostasis in cells, may become cytotoxic instead of cytoprotective, triggering some unique signaling transduction mechanisms [35]. CHOP is also known as growth arrest- and DNA damage-inducible gene 153 (GADD153) or DNA damage-inducible transcript 3 [DDIT3]), which contains an element for the positive regulation of the mitochondrial UPS [36]. Following the failure to restore ER protein homeostasis, the prolonged activation of the UPS may initiate the apoptotic cell death by up-regulating CHOP [37]. Being a master regulator with a pivotal role in the adaptation to stresses, ATF4 is both a necessity and sufficiency for the ER stress-induced upregulated expression of regulated in development and DNA damage response 1 (REDD1), a gene transcriptionally upregulated during ER stress [38, 39]. PERK, serving as the ER stress sensor and mediator of the UPR, is known to mediate the cell death as well [40, 41]. When it comes to the association of KDM1A with both ROS and ER stress, it shouldn't be neglected that RN-1, a known inhibitor of KDM1A, diminishes the content of ROS in a murine model of sickle cell disease (SCD) and that the therapeutic targeting of KDM1A in Ewing sarcoma engages the ER stress response [42, 43]. Existing research has furthermore highlighted the role of excessive ROS generation and ER stress in the

induction of apoptosis of OS cells [44, 45]. Based on these perspectives, we additionally confirmed that the overexpression of KDM1A in OS cells may result in the diminished apoptosis within via inhibiting the excessive ROS generation and aggravating the ER stress, along with the decreased levels of ER stress-related factors CHOP, ATF4 and PERK. However, we should use KDM1A inhibitor such as RN-1 to verify the effect of KDM1A in OS cells in the future.

DNA demethylation, which is defined as the enzymatic process which results in the removal of the methyl group from 5-methylcytosine (5meC) via destroying the carbon-carbon bond [46, 47]. Increasing research has highlighted the role of site-specific DNA demethylation as a possible target for the epigenetic therapy of tumor, like OS [12, 48]. More importantly, some key regulators in OS have been revealed based on the integrated genome-wide methylation and expression analysis [49]. Like we mentioned earlier, KDMI1A, being a demethylase, unleashed its inhibitory effect on the expression of CDH-1 [18, 19]. Considering this, we have the reason to believe that there must exist other candidate(s) that could be demethylated by KDM1A and participated in the underlying mechanism by which KDM1A exerted its effects on OS. Upon seeking the candidate(s), Bcl-2 and c-Myc caught our attention in that they have been widely reported to participate in different malignancies, OS, for instance [6, 7]. What really surprised us is the fact that KDM1A knockdown, in response to the stimulation of estrogen, caused the abrogated expressions of Bcl-2 and c-Myc genes, based on the relevant data in Reactome database (https://reactome.org/content/detail/R-HSA-9011984) [50-53]. Bcl-2 and c-Myc are some of the related proteins arguably amongst the most widely investigated in all of biology, where it has been indicated that Bcl-2 itself is a faction within the Bcl-2 family

which is known as the “Bcl-2-like” pro-survival proteins, while c-Myc, plays a predominant role in the apoptosis and shows a co-operativity with Bcl-2 [54]. Considering these, we have the strong belief that KDM1A may demethylate Bcl-2/c-Myc in OS cells MG-63 and inversely, Bcl-2/c-Myc may be implicated in the mechanism underlying the effects of KDM1A in OS. Here, such belief of us was reconfirmed in OS cells where KDM1A demethylate Bcl-2/c-Myc in an H3K9-dependent manner and the silence of both Bcl-2/c-Myc not only produced contrary results to those following the overexpression of KDM1A but also reversed the effects of overexpressed KDM1A in both ROS generation and ER stress of OS cells. Based on these, a safe conclusion could be drawn that KDM1A overexpression, opposite to its knockdown, may restrain the ROS generation and ER stress so as to repress the apoptosis of OS cells, the mechanism of which may be associated with the demethylation of Bcl-2/c-Myc.

Conclusion

Collectively, linking these investigations together [7, 18], we came up with a novel discovery where the participation of KDM1A as a demethylase in OS has been re-evaluated and KDM1A-mediated demethylation of Bcl-2/c-Myc may regulate the ROS generation and ER stress in OS cells MG-63 cells. However, it’s worth noting that despite the emphasis on the effects of KDM1A/Bcl-2/c-Myc on the apoptosis of OS cells from the perspectives of ROS generation and ER stress in our current research, some other mechanisms, DNA damage, for instance, may implicated in the apoptosis of OS cells as well, as evidenced by the discoveries highlighting the induction of DNA damage on the apoptosis and the recruitment of KDM1A to the sites of DNA damage [55, 56]. Also, we only used one OS cell line MG-63 in our current research and it remained vague whether

same results could be concluded from other OS cells *in vitro*. These mysteries, accordingly, will be solved in our future research as appropriate.

Funding

This study was supported by the 2021 Zhejiang Provincial Health Science and Technology Program Project (Study on the inhibition effect and mechanism of siRNA bcl-2 and siRNA c-myc genes co-transfection on MG-63 in human osteosarcoma resistant cells) [2021KY939].

Declaration of interest

The authors declare no conflicts of interest.

Data Availability Statement

The datasets generated during and/or analyzed during the current study are available from the corresponding author on reasonable request.

Authors' contributions

Substantial contributions to conception and design: Xuezheng Zhao and Lijun Li

Data acquisition, data analysis and interpretation: Sihua Zheng, Baoyong Tang, Yebing Zhang, Wei Gao

Drafting the article or critically revising it for important intellectual content: Xuezheng Zhao, Lijun Li, Sihua Zheng, Baoyong Tang, Yebing Zhang, Wei Gao

Final approval of the version to be published: All authors

Agreement to be accountable for all aspects of the work in ensuring that questions related to the accuracy or integrity of the work are appropriately investigated and resolved: Xuezheng Zhao, Lijun Li, Sihua Zheng, Baoyong Tang, Yebing Zhang, Wei Gao

Acknowledgments

Not applicable.

References

1. Eaton BR, Schwarz R, Vatner R, Yeh B, Claude L, Indelicato DJ, et al. Osteosarcoma. Pediatric blood & cancer. 2021 May;68 Suppl 2:e28352. PubMed PMID: 32779875. Epub 2020/08/12. eng.

2. Chen C, Xie L, Ren T, Huang Y, Xu J, Guo W. Immunotherapy for osteosarcoma: Fundamental mechanism, rationale, and recent breakthroughs. Cancer letters. 2021 Mar 1;500:1-10. PubMed PMID: 33359211. Epub 2020/12/29. eng.

3. Yoshida A. Osteosarcoma: Old and New Challenges. Surgical pathology clinics. 2021 Dec;14(4):567-83. PubMed PMID: 34742481. Epub 2021/11/08. eng.

4. Ghafouri-Fard S, Shirvani-Farsani Z, Hussen BM, Taheri M. The critical roles of lncRNAs in the development of osteosarcoma. Biomedicine & pharmacotherapy = Biomedecine & pharmacotherapie. 2021 Mar;135:111217. PubMed PMID: 33433358. Epub 2021/01/13. eng.

5. Chen Y, Liu R, Wang W, Wang C, Zhang N, Shao X, et al. Advances in targeted therapy for osteosarcoma based on molecular classification. Pharmacological research. 2021 Jul;169:105684. PubMed PMID: 34022396. Epub 2021/05/23. eng.

6. Ozdek A, Sarac S, Akyol MU, Sungur A, Yilmaz T. c-myc and bcl-2 Expression in supraglottic squamous cell carcinoma of the larynx. Otolaryngology--head and neck surgery : official journal of American Academy of Otolaryngology-Head and Neck Surgery. 2004 Jul;131(1):77-83. PubMed PMID: 15243561. Epub 2004/07/10. eng.

7. Wu X, Cai ZD, Lou LM, Zhu YB. Expressions of p53, c-MYC, BCL-2 and apoptotic index in human osteosarcoma and their correlations with prognosis of patients. Cancer epidemiology. 2012 Apr;36(2):212-6. PubMed PMID: 21890444. Epub 2011/09/06. eng.

8. Du X, Fu X, Yao K, Lan Z, Xu H, Cui Q, et al. Bcl-2 delays cell cycle through mitochondrial ATP and ROS. Cell cycle (Georgetown, Tex). 2017 Apr 3;16(7):707-13. PubMed PMID: 28278051. Pubmed Central PMCID: PMC5397261. Epub 2017/03/10. eng.

9. Yang S, Zhou F, Dong Y, Ren F. α-Mangostin Induces Apoptosis in Human Osteosarcoma Cells Through ROS-Mediated Endoplasmic Reticulum Stress via the WNT Pathway. Cell transplantation. 2021 Jan-Dec;30:9636897211035080. PubMed PMID: 34318699. Pubmed Central PMCID: PMC8323427. Epub 2021/07/29. eng.

10. DeNicola GM, Karreth FA, Humpton TJ, Gopinathan A, Wei C, Frese K, et al. Oncogene-induced Nrf2 transcription promotes ROS detoxification and tumorigenesis. Nature. 2011 Jul 6;475(7354):106-9. PubMed PMID: 21734707. Pubmed Central PMCID: PMC3404470. Epub 2011/07/08. eng.

11. Feng W, Dean DC, Hornicek FJ, Spentzos D, Hoffman RM, Shi H, et al. Myc is a

prognostic biomarker and potential therapeutic target in osteosarcoma. Therapeutic advances in medical oncology. 2020;12:1758835920922055. PubMed PMID: 32426053. Pubmed Central PMCID: PMC7222246. Epub 2020/05/20. eng.

12. Asano N, Takeshima H, Yamashita S, Takamatsu H, Hattori N, Kubo T, et al. Epigenetic reprogramming underlies efficacy of DNA demethylation therapy in osteosarcomas. Scientific reports. 2019 Dec 30;9(1):20360. PubMed PMID: 31889115. Pubmed Central PMCID: PMC6937291. Epub 2020/01/01. eng.

13. Xu J, Li D, Cai Z, Zhang Y, Huang Y, Su B, et al. An integrative analysis of DNA methylation in osteosarcoma. Journal of bone oncology. 2017 Nov;9:34-40. PubMed PMID: 29234590. Pubmed Central PMCID: PMC5715438. Epub 2017/12/14. eng.

14. Chen XG, Ma L, Xu JX. Abnormal DNA methylation may contribute to the progression of osteosarcoma. Molecular medicine reports. 2018 Jan;17(1):193-9. PubMed PMID: 29115427. Pubmed Central PMCID: PMC5780126. Epub 2017/11/09. eng.

15. Perillo B, Tramontano A, Pezone A, Migliaccio A. LSD1: more than demethylation of histone lysine residues. Experimental & molecular medicine. 2020 Dec;52(12):1936-47. PubMed PMID: 33318631. Pubmed Central PMCID: PMC8080763. Epub 2020/12/16. eng.

16. Gu F, Lin Y, Wang Z, Wu X, Ye Z, Wang Y, et al. Biological roles of LSD1 beyond its demethylase activity. Cellular and molecular life sciences : CMLS. 2020 Sep;77(17):3341-50. PubMed PMID: 32193608. Epub 2020/03/21. eng.

17. Shao G, Wan X, Lai W, Wu C, Jin J, Liu X, et al. Inhibition of lysine-specific demethylase 1 prevents proliferation and mediates cisplatin sensitivity in ovarian cancer cells. Oncology letters. 2018 Jun;15(6):9025-32. PubMed PMID: 29928330. Pubmed Central PMCID: Pmc6004655. Epub 2018/06/22. eng.

18. Bennani-Baiti IM, Machado I, Llombart-Bosch A, Kovar H. Lysine-specific demethylase 1 (LSD1/KDM1A/AOF2/BHC110) is expressed and is an epigenetic drug target in chondrosarcoma, Ewing's sarcoma, osteosarcoma, and rhabdomyosarcoma. Human pathology. 2012 Aug;43(8):1300-7. PubMed PMID: 22245111. Epub 2012/01/17. eng.

19. Miao Y, Liu G, Liu L. Histone methyltransferase SUV39H2 regulates LSD1-dependent CDH1 expression and promotes epithelial mesenchymal transition of osteosarcoma. Cancer cell international. 2021 Jan 4;21(1):2. PubMed PMID: 33397384. Pubmed Central PMCID: PMC7784292. Epub 2021/01/06. eng.

20. Mikulčić M, Tabrizi-Wizsy NG, Bernhart EM, Asslaber M, Trummer C, Windischhofer W, et al. 15d-PGJ(2) Promotes ROS-Dependent Activation of MAPK-Induced Early Apoptosis in Osteosarcoma Cell In Vitro and in an Ex Ovo CAM Assay. International journal of molecular

463 sciences. 2021 Oct 29;22(21). PubMed PMID: 34769194. Pubmed Central PMCID:
464 PMC8583949. Epub 2021/11/14. eng.
465 21. Hou X, Li Q, Yang L, Yang Z, He J, Li Q, et al. KDM1A and KDM3A promote tumor
466 growth by upregulating cell cycle-associated genes in pancreatic cancer. Experimental biology
467 and medicine (Maywood, NJ). 2021 Sep;246(17):1869-83. PubMed PMID: 34171978. Pubmed
468 Central PMCID: PMC8424634. Epub 2021/06/27. eng.
469 22. Livak KJ, Schmittgen TD. Analysis of relative gene expression data using real-time
470 quantitative PCR and the 2(-Delta Delta C(T)) Method. Methods (San Diego, Calif). 2001
471 Dec;25(4):402-8. PubMed PMID: 11846609. Epub 2002/02/16. eng.
472 23. Shimizu T, Kamel WA, Yamaguchi-Iwai S, Fukuchi Y, Muto A, Saya H. Calcitriol exerts
473 an anti-tumor effect in osteosarcoma by inducing the endoplasmic reticulum stress response.
474 Cancer science. 2017 Sep;108(9):1793-802. PubMed PMID: 28643892. Pubmed Central PMCID:
475 PMC5581526. Epub 2017/06/24. eng.
476 24. Sun X, Gu X, Li H, Xu P, Li M, Zhu Y, et al. H3K9me2 regulates early transcription
477 factors to promote mesenchymal stem-cell differentiation into cardiomyocytes. Molecular
478 medicine reports. 2021 Aug;24(2). PubMed PMID: 34184085. Epub 2021/06/30. eng.
479 25. Fang Y, Liao G, Yu B. LSD1/KDM1A inhibitors in clinical trials: advances and prospects.
480 Journal of hematology & oncology. 2019 Dec 4;12(1):129. PubMed PMID: 31801559. Pubmed
481 Central PMCID: PMC6894138. Epub 2019/12/06. eng.
482 26. Ambrosio S, Saccà CD, Majello B. Epigenetic regulation of epithelial to mesenchymal
483 transition by the Lysine-specific demethylase LSD1/KDM1A. Biochimica et biophysica acta
484 Gene regulatory mechanisms. 2017 Sep;1860(9):905-10. PubMed PMID: 28720390. Epub
485 2017/07/20. eng.
486 27. Karakaidos P, Verigos J, Magklara A. LSD1/KDM1A, a Gate-Keeper of Cancer Stemness
487 and a Promising Therapeutic Target. Cancers. 2019 Nov 20;11(12). PubMed PMID: 31756917.
488 Pubmed Central PMCID: PMC6966601. Epub 2019/11/24. eng.
489 28. Huang M, Chen C, Geng J, Han D, Wang T, Xie T, et al. Targeting KDM1A attenuates
490 Wnt/β-catenin signaling pathway to eliminate sorafenib-resistant stem-like cells in hepatocellular
491 carcinoma. Cancer letters. 2017 Jul 10;398:12-21. PubMed PMID: 28377178. Epub 2017/04/06.
492 eng.
493 29. Wan Y, Yang L, Jiang S, Qian D, Duan J. Excessive Apoptosis in Ulcerative Colitis:
494 Crosstalk Between Apoptosis, ROS, ER Stress, and Intestinal Homeostasis. Inflammatory bowel
495 diseases. 2022 Mar 30;28(4):639-48. PubMed PMID: 34871402. Epub 2021/12/07. eng.
496 30. Simon HU, Haj-Yehia A, Levi-Schaffer F. Role of reactive oxygen species (ROS) in

apoptosis induction. Apoptosis : an international journal on programmed cell death. 2000 Nov;5(5):415-8. PubMed PMID: 11256882. Epub 2001/03/21. eng.

31. Zhuang C, Ni S, Yang ZC, Liu RP. Oxidative Stress Induces Chondrocyte Apoptosis through Caspase-Dependent and Caspase-Independent Mitochondrial Pathways and the Antioxidant Mechanism of Angelica Sinensis Polysaccharide. Oxidative medicine and cellular longevity. 2020;2020:3240820. PubMed PMID: 33224431. Pubmed Central PMCID: PMC7669361. Epub 2020/11/24. eng.

32. Rowe LA, Degtyareva N, Doetsch PW. DNA damage-induced reactive oxygen species (ROS) stress response in Saccharomyces cerevisiae. Free radical biology & medicine. 2008 Oct 15;45(8):1167-77. PubMed PMID: 18708137. Pubmed Central PMCID: PMC2643028. Epub 2008/08/19. eng.

33. Prasad S, Gupta SC, Tyagi AK. Reactive oxygen species (ROS) and cancer: Role of antioxidative nutraceuticals. Cancer letters. 2017 Feb 28;387:95-105. PubMed PMID: 27037062. Epub 2016/04/03. eng.

34. Lin H, Peng Y, Li J, Wang Z, Chen S, Qing X, et al. Reactive Oxygen Species Regulate Endoplasmic Reticulum Stress and ER-Mitochondrial Ca(2+) Crosstalk to Promote Programmed Necrosis of Rat Nucleus Pulposus Cells under Compression. Oxidative medicine and cellular longevity. 2021;2021:8810698. PubMed PMID: 33815661. Pubmed Central PMCID: PMC7987452 publication of this paper. Epub 2021/04/06. eng.

35. Zeeshan HM, Lee GH, Kim HR, Chae HJ. Endoplasmic Reticulum Stress and Associated ROS. International journal of molecular sciences. 2016 Mar 2;17(3):327. PubMed PMID: 26950115. Pubmed Central PMCID: PMC4813189. Epub 2016/03/08. eng.

36. Horibe T, Hoogenraad NJ. The chop gene contains an element for the positive regulation of the mitochondrial unfolded protein response. PloS one. 2007 Sep 12;2(9):e835. PubMed PMID: 17848986. Pubmed Central PMCID: PMC1950685. Epub 2007/09/13. eng.

37. Hu H, Tian M, Ding C, Yu S. The C/EBP Homologous Protein (CHOP) Transcription Factor Functions in Endoplasmic Reticulum Stress-Induced Apoptosis and Microbial Infection. Frontiers in immunology. 2018;9:3083. PubMed PMID: 30662442. Pubmed Central PMCID: PMC6328441. Epub 2019/01/22. eng.

38. Wortel IMN, van der Meer LT, Kilberg MS, van Leeuwen FN. Surviving Stress: Modulation of ATF4-Mediated Stress Responses in Normal and Malignant Cells. Trends in endocrinology and metabolism: TEM. 2017 Nov;28(11):794-806. PubMed PMID: 28797581. Pubmed Central PMCID: PMC5951684. Epub 2017/08/12. eng.

39. B'Chir W, Maurin AC, Carraro V, Averous J, Jousse C, Muranishi Y, et al. The

eIF2α/ATF4 pathway is essential for stress-induced autophagy gene expression. Nucleic acids research. 2013 Sep;41(16):7683-99. PubMed PMID: 23804767. Pubmed Central PMCID: PMC3763548. Epub 2013/06/28. eng.

40. van Vliet AR, Giordano F, Gerlo S, Segura I, Van Eygen S, Molenberghs G, et al. The ER Stress Sensor PERK Coordinates ER-Plasma Membrane Contact Site Formation through Interaction with Filamin-A and F-Actin Remodeling. Molecular cell. 2017 Mar 2;65(5):885-99.e6. PubMed PMID: 28238652. Epub 2017/02/28. eng.

41. Dadey DYA, Kapoor V, Khudanyan A, Thotala D, Hallahan DE. PERK Regulates Glioblastoma Sensitivity to ER Stress Although Promoting Radiation Resistance. Molecular cancer research : MCR. 2018 Oct;16(10):1447-53. PubMed PMID: 29991528. Epub 2018/07/12. eng.

42. Rivers A, Jagadeeswaran R, Lavelle D. Potential role of LSD1 inhibitors in the treatment of sickle cell disease: a review of preclinical animal model data. American journal of physiology Regulatory, integrative and comparative physiology. 2018 Oct 1;315(4):R840-r7. PubMed PMID: 30067082. Pubmed Central PMCID: PMC6734057. Epub 2018/08/02. eng.

43. Pishas KI, Drenberg CD, Taslim C, Theisen ER, Johnson KM, Saund RS, et al. Therapeutic Targeting of KDM1A/LSD1 in Ewing Sarcoma with SP-2509 Engages the Endoplasmic Reticulum Stress Response. Molecular cancer therapeutics. 2018 Sep;17(9):1902-16. PubMed PMID: 29997151. Pubmed Central PMCID: PMC6201274. Epub 2018/07/13. eng.

44. Wang S, Li H, Chen S, Wang Z, Yao Y, Chen T, et al. Andrographolide induces apoptosis in human osteosarcoma cells via the ROS/JNK pathway. International journal of oncology. 2020 Jun;56(6):1417-28. PubMed PMID: 32236589. Pubmed Central PMCID: PMC7170044. Epub 2020/04/03. eng.

45. Wang GS, Chen JY, Chen WC, Wei IC, Lin SW, Liao KW, et al. Surfactin induces ER stress-mediated apoptosis via IRE1-ASK1-JNK signaling in human osteosarcoma. Environmental toxicology. 2022 Mar;37(3):574-84. PubMed PMID: 34850538. Epub 2021/12/02. eng.

46. Bochtler M, Kolano A, Xu GL. DNA demethylation pathways: Additional players and regulators. BioEssays : news and reviews in molecular, cellular and developmental biology. 2017 Jan;39(1):1-13. PubMed PMID: 27859411. Epub 2016/11/20. eng.

47. Wu SC, Zhang Y. Active DNA demethylation: many roads lead to Rome. Nature reviews Molecular cell biology. 2010 Sep;11(9):607-20. PubMed PMID: 20683471. Pubmed Central PMCID: PMC3711520. Epub 2010/08/05. eng.

48. Neja SA. Site-Specific DNA Demethylation as a Potential Target for Cancer Epigenetic Therapy. Epigenetics insights. 2020;13:2516865720964808. PubMed PMID: 35036833. Pubmed

Central PMCID: PMC8756105. Epub 2020/10/21. eng.

49. Wang F, Qin G, Liu J, Wang X, Ye B. Integrated Genome-Wide Methylation and Expression Analyses Reveal Key Regulators in Osteosarcoma. Computational and mathematical methods in medicine. 2020;2020:7067649. PubMed PMID: 32855654. Pubmed Central PMCID: PMC7443031. Epub 2020/08/29. eng.

50. Perillo B, Ombra MN, Bertoni A, Cuozzo C, Sacchetti S, Sasso A, et al. DNA oxidation as triggered by H3K9me2 demethylation drives estrogen-induced gene expression. Science (New York, NY). 2008 Jan 11;319(5860):202-6. PubMed PMID: 18187655. Epub 2008/01/12. eng.

51. Wissmann M, Yin N, Müller JM, Greschik H, Fodor BD, Jenuwein T, et al. Cooperative demethylation by JMJD2C and LSD1 promotes androgen receptor-dependent gene expression. Nature cell biology. 2007 Mar;9(3):347-53. PubMed PMID: 17277772. Epub 2007/02/06. eng.

52. Wang J, Hevi S, Kurash JK, Lei H, Gay F, Bajko J, et al. The lysine demethylase LSD1 (KDM1) is required for maintenance of global DNA methylation. Nature genetics. 2009 Jan;41(1):125-9. PubMed PMID: 19098913. Epub 2008/12/23. eng.

53. Su CH, Tzeng TY, Cheng C, Hsu MT. An H2A histone isotype regulates estrogen receptor target genes by mediating enhancer-promoter-3'-UTR interactions in breast cancer cells. Nucleic acids research. 2014 Mar;42(5):3073-88. PubMed PMID: 24371278. Pubmed Central PMCID: PMC3950719. Epub 2013/12/29. eng.

54. Fairlie WD, Lee EF. Co-Operativity between MYC and BCL-2 Pro-Survival Proteins in Cancer. International journal of molecular sciences. 2021 Mar 11;22(6). PubMed PMID: 33799592. Pubmed Central PMCID: PMC8000576. Epub 2021/04/04. eng.

55. Norbury CJ, Zhivotovsky B. DNA damage-induced apoptosis. Oncogene. 2004 Apr 12;23(16):2797-808. PubMed PMID: 15077143. Epub 2004/04/13. eng.

56. Mosammaparast N, Kim H, Laurent B, Zhao Y, Lim HJ, Majid MC, et al. The histone demethylase LSD1/KDM1A promotes the DNA damage response. The Journal of cell biology. 2013 Nov 11;203(3):457-70. PubMed PMID: 24217620. Pubmed Central PMCID: PMC3824007. Epub 2013/11/13. eng.

Figure legends

Figure 1. KDM1A overexpression promoted ROS generation and apoptosis yet inhibited the viability of OS cells MG-63, while its knockdown led to contrary results.

First, the overexpression plasmid of KDM1A (presented as KDM1A in the figures) and shRNA against KDM1A (stylized as shKDM1A) were transfected into OS cells MG-63 to reveal the effects of KDM1A on the malignant behaviors of OS cells. (A) The transfection was proved to be successful, as reflected by the results of reverse-transcription quantitative PCR, with GAPDH as the housekeeping control. (B-D) Meanwhile, based on the MTT (B) and flow cytometry assay (C-D), the effects of KDM1A knockdown or overexpression on the viability at 48 h and the apoptosis in MG-63 cells were evaluated. (E) The production of ROS in MG-63 cells with either the knockdown or the overexpression of KDM1A was calculated in the end.

All data of three independent tests were expressed as mean ± standard deviation.

$^{***}p<0.001$, vs. shNC; $^{\wedge}p<0.05$, $^{\wedge\wedge}p<0.01$, $^{\wedge\wedge\wedge}p<0.001$, vs. NC.

Abbreviation: KDM1A: lysine demethylase 1A; shRNA: short hairpin RNA; NC: negative control; OS: osteosarcoma; ROS: reactive oxygen species; MTT: 3-[4,5-dimethylthiazol-2-yl]-2,5 diphenyl tetrazolium bromide; h: hour.

Figure 2. Effects of KDM1A knockdown/overexpression on the ER stress and the expressions of Bcl-2/MYC in OS cells MG-63.

Likewise, the significant roles of ER stress and Bcl-2/MYC in OS cells has been emphasized. (A-B) Herein, some ER stress-related factors were measured, including CHOP, PERK, and ATF4, based on the assay of western blot, with GAPDH as the

housekeeping control. (C-F) Meanwhile, the protein and mRNA levels of Bcl-2/MYC were quantified via western blot (C-D) and reverse-transcription quantitative PCR (E-F), with GAPDH as the housekeeping control.

All data of three independent tests were expressed as mean ± standard deviation.

$^{**}p<0.01$, $^{***}p<0.001$, vs. shNC; $^{\wedge\wedge\wedge}p<0.001$, vs. NC.

Abbreviation: ER: endoplasmic reticulum; CHOP: C/EBP homologous protein; PERK: proline-rich extensin-like receptor kinase; ATF4: activating transcription factor 4; Bcl-2: B-cell lymphoma-2; MYC: cellular-Myc.

Figure 3. Analysis of KDM1A/Bcl-2/MYC axis on OS cells.

(A-D) ChIP-PCR analysis was performed to determine the enrichment of Bcl-2/MYC promoter using the antibody against KDM1A or H3K9me2. (E-F) Evaluation of transfection efficiency of Bcl-2/MYC siRNA via and reverse-transcription quantitative PCR, with GAPDH as the housekeeping control. (G-H) Interplay between KDM1A and Bcl-2/MYC on the ROS production in OS cells MG-63.

All data of three independent tests were expressed as mean ± standard deviation.

$^{**}p<0.01$, $^{***}p<0.001$, vs. shNC; $^{++}p<0.01$, $^{+++}p<0.001$, vs. siNC; $^{\#}p<0.05$, $^{\#\#}p<0.01$, $^{\#\#\#}p<0.001$, vs. NC+shNC; $^{\Delta\Delta\Delta}p<0.001$, vs. siNC+KDM1A; $^{\&\&\&}p<0.001$, vs. siBcl-2+NC; $^{\ddagger\ddagger\ddagger}p<0.001$, vs. siMYC+NC.

Abbreviation: ChIP-PCR: chromatin immunoprecipitation-PCR.

Figure 4. Evaluation of KDM1A/Bcl-2/MYC axis on the ER stress in OS cells.

(A-D) As to the protein expression of ER stress-related factors CHOP (B), PERK (C), and ATF4 (D) in OS cells MG-63, their levels following the silence of Bcl-2/MYC and the overexpression of KDM1A were determined via western blot. GAPDH was the

housekeeping control used.

All data of three independent tests were expressed as mean ± standard deviation. $^{\#\#}p<0.01$, $^{\#\#\#}p<0.001$, vs. NC+siNC; $^{\Delta\Delta}p<0.01$, $^{\Delta\Delta\Delta}p<0.001$, vs. siNC+KDM1A; $^{\&\&}p<0.01$, $^{\&\&\&}p<0.001$, vs. siBcl-2+NC; $^{\ddagger\ddagger}p<0.01$, $^{\ddagger\ddagger\ddagger}p<0.001$, vs. siMYC+NC.

Figure 5. Determination of KDM1A/Bcl-2/MYC axis on the apoptosis in OS cells.

(A-D) The apoptosis rates of OS cells MG-63 following the silence of Bcl-2/MYC and the overexpression of KDM1A were calculated with the help of flow cytometry.

All data of three independent tests were expressed as mean ± standard deviation. $^{\#}p<0.05$, $^{\#\#}p<0.01$, $^{\#\#\#}p<0.001$, vs. NC+siNC; $^{\Delta\Delta\Delta}p<0.001$, vs. siNC+KDM1A; $^{\&\&\&}p<0.001$, vs. siBcl-2+NC; $^{\ddagger\ddagger\ddagger}p<0.001$, vs. siMYC+NC.

Tables

Table 1.

Table 1. Sequences for transfection

Gene	Target sequence (5’-3’)
shKDM1A	CTCTCAGAAGATGAGTATTAT
shNC	CATGTCTCAGAAGATAGTATT
siBcl-2#1	ATCTGGAAATCCTCCTAATTTTT
siBcl-2#2	TGGAAATCCTCCTAATTTTTACT
siBcl-2#3	CTGATTCATTGGGAAGTTTCAAA
siMYC#1	CTGCTTAGACGCTGGATTTTTTT
siMYC#2	TGCTTAGACGCTGGATTTTTTTC
siMYC#3	GAGGAAGAAATCGATGTTGTTTC
siNC	CTGAAGGATTCATTCAGAAGTTT

Table 2.

Table 2. Sequences of Primers

Gene	Primer sequence (5’-3’)	
	Forward	Reverse
Bcl-2	GATGACTGAGTACCTGAACC	AGCAGAGTCTTCAGAGACAG
MYC	GTAGTGGAAAACCAGCAG	CTCTTTTCCACAGAAACAAC
KDM1A	CACAGTTATTTAGAGCGTCA	CTTTCTCTTTAGGAACCTTG
GAPDH	ATTGACCTCAACTACATGGT	CATACTTCTCATGGTTCACA

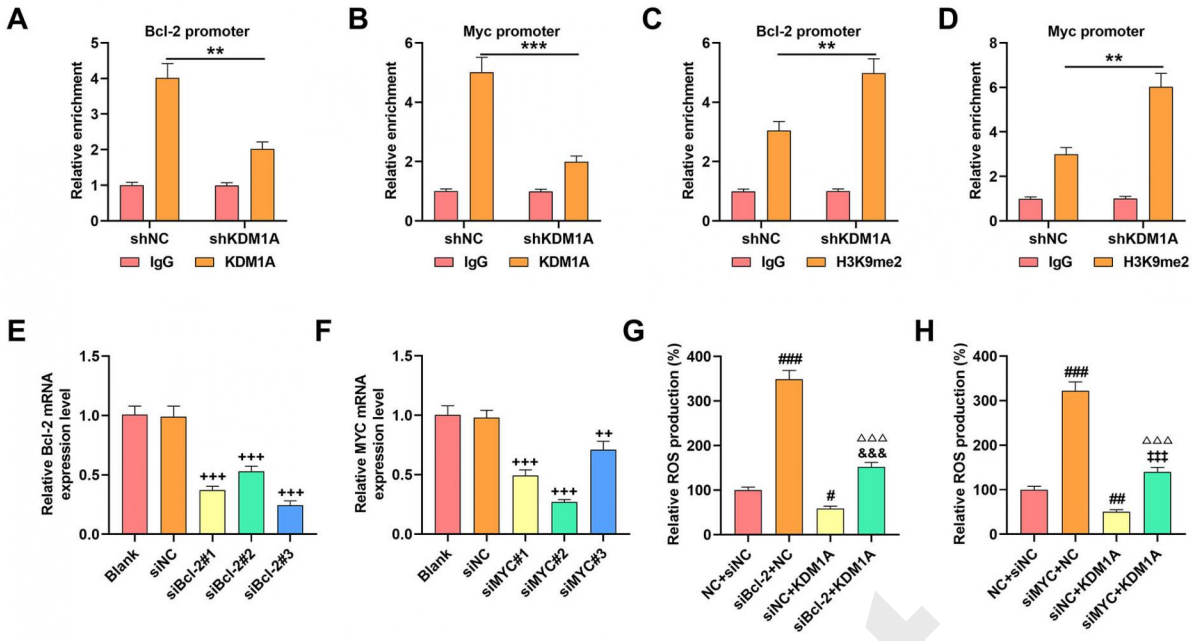
A
Bcl-2 promoter
Relative enrichment
**
shNC
shKDM1A
IgG
KDM1A
B
Myc promoter
***
C
Bcl-2 promoter
H3K9me2
D
Myc promoter
E
Relative Bcl-2 mRNA expression level
Blank
siNC
siBcl-2#1
siBcl-2#2
siBcl-2#3
F
Relative MYC mRNA expression level
siMYC#1
siMYC#2
siMYC#3
G
Relative ROS production (%)
NC+siNC
siBcl-2+NC
siNC+KDM1A
siBcl-2+KDM1A
H
siMYC+NC
siMYC+KDM1A

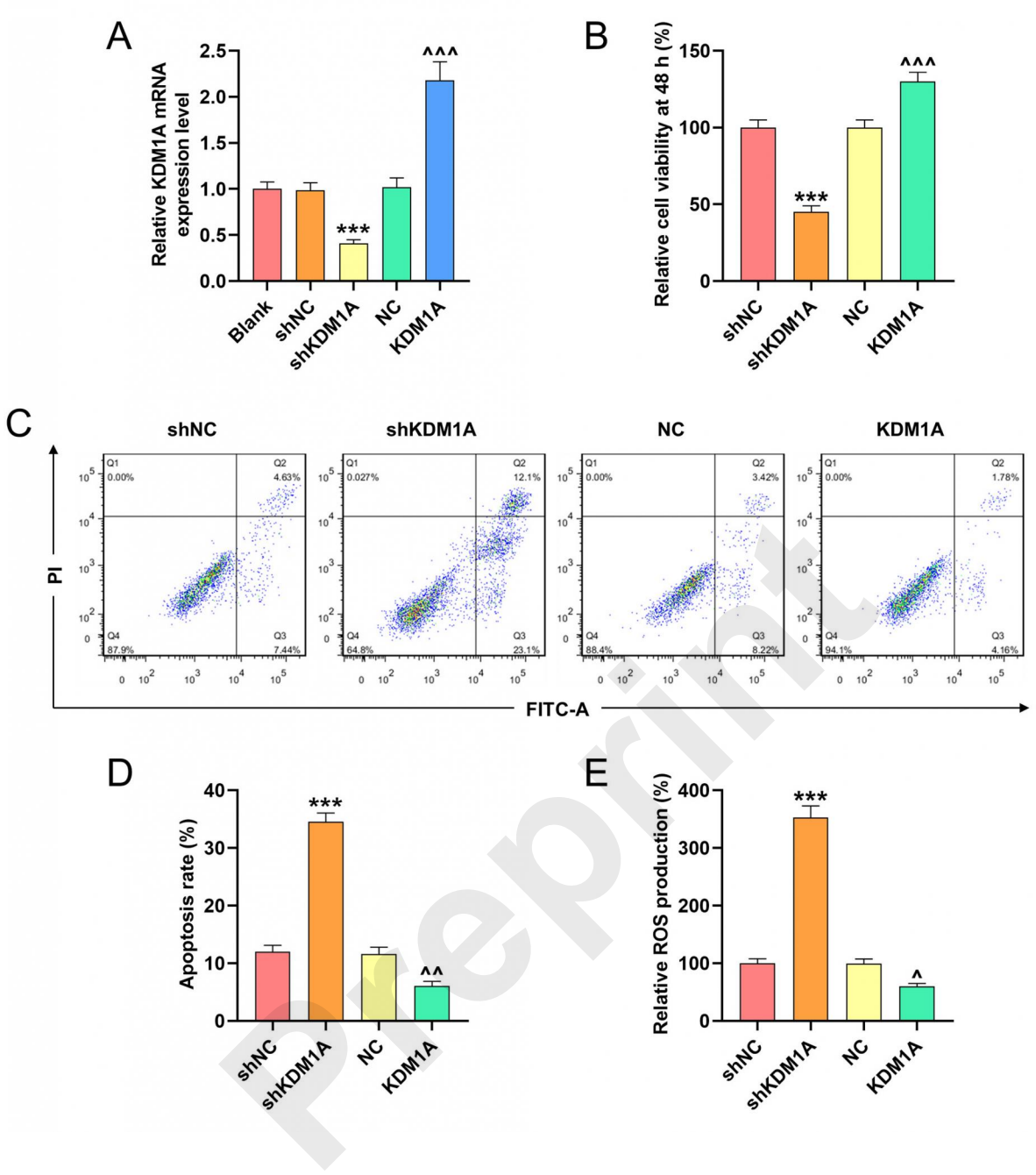
A
Relative KDM1A mRNA expression level
2.5
2.0
1.5
1.0
0.5
0.0
***
^^^
Blank
shNC
shKDM1A
NC
KDM1A
B
Relative cell viability at 48 h (%)
150
100
50
0
***
^^^
shNC
shKDM1A
NC
KDM1A
C
shNC
shKDM1A
NC
KDM1A
PI
FITC-A
Q1 0.00%
Q2 4.63%
Q4 87.9%
Q3 7.44%
Q1 0.027%
Q2 12.1%
Q4 64.8%
Q3 23.1%
Q1 0.00%
Q2 3.42%
Q4 88.4%
Q3 8.22%
Q1 0.00%
Q2 1.78%
Q4 94.1%
Q3 4.16%
D
Apoptosis rate (%)
40
30
20
10
0
***
^^
shNC
shKDM1A
NC
KDM1A
E
Relative ROS production (%)
400
300
200
100
0
***
^
shNC
shKDM1A
NC
KDM1A

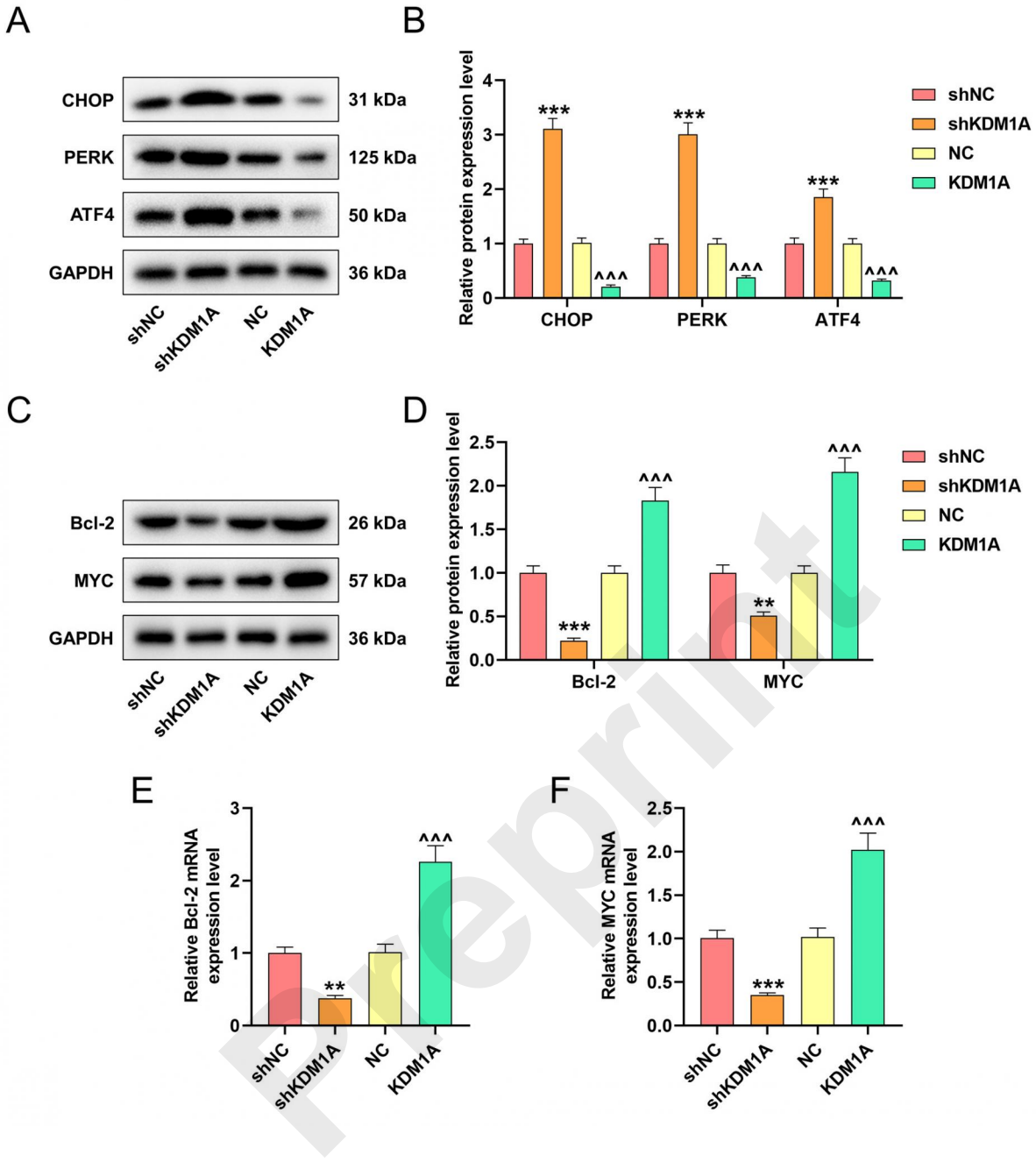
A
CHOP
PERK
ATF4
GAPDH
31 kDa
125 kDa
50 kDa
36 kDa
shNC
shKDM1A
NC
KDM1A
B
Relative protein expression level
CHOP
PERK
ATF4
shNC
shKDM1A
NC
KDM1A
C
Bcl-2
MYC
GAPDH
26 kDa
57 kDa
36 kDa
D
Relative protein expression level
Bcl-2
MYC
E
Relative Bcl-2 mRNA expression level
F
Relative MYC mRNA expression level

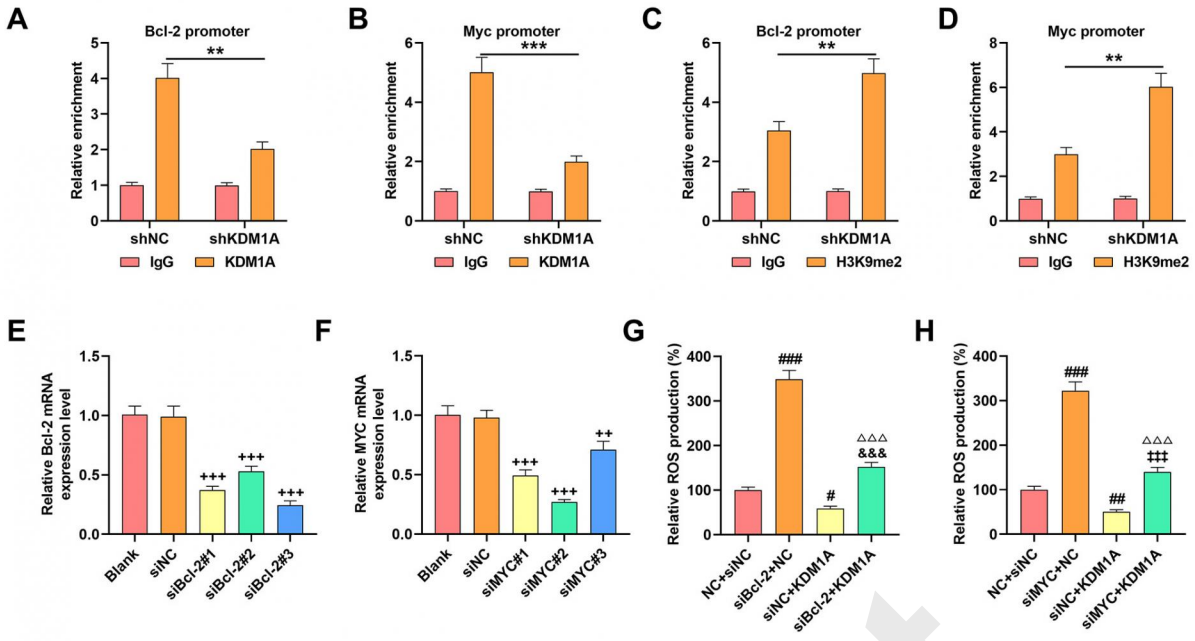
A
Bcl-2 promoter
Relative enrichment
**
shNC
shKDM1A
IgG
KDM1A
B
Myc promoter
***
C
Bcl-2 promoter
H3K9me2
D
Myc promoter
E
Relative Bcl-2 mRNA expression level
Blank
siNC
siBcl-2#1
siBcl-2#2
siBcl-2#3
F
Relative MYC mRNA expression level
siMYC#1
siMYC#2
siMYC#3
G
Relative ROS production (%)
NC+siNC
siBcl-2+NC
siNC+KDM1A
siBcl-2+KDM1A
H
siMYC+NC
siMYC+KDM1A

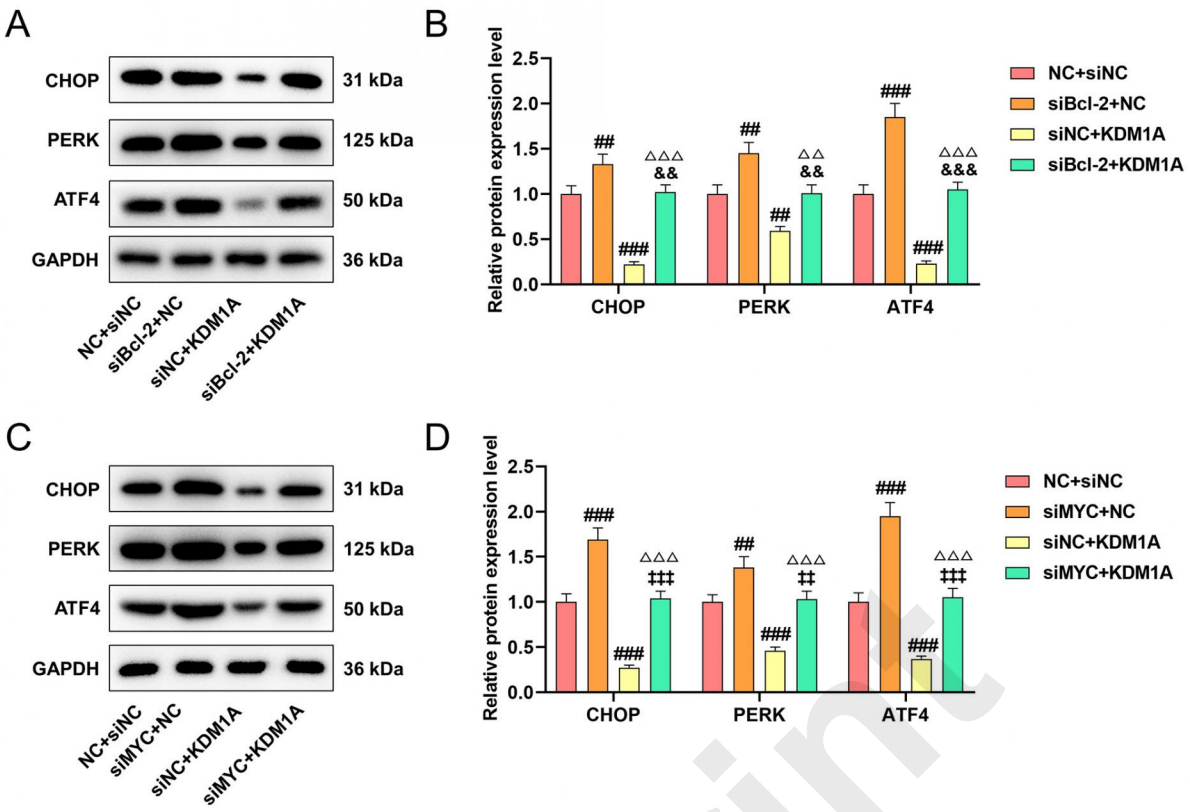
A
CHOP
PERK
ATF4
GAPDH
31 kDa
125 kDa
50 kDa
36 kDa
NC+siNC
siBcl-2+NC
siNC+KDM1A
siBcl-2+KDM1A
B
Relative protein expression level
2.5
2.0
1.5
1.0
0.5
0.0
CHOP
PERK
ATF4
NC+siNC
siBcl-2+NC
siNC+KDM1A
siBcl-2+KDM1A
C
CHOP
PERK
ATF4
GAPDH
31 kDa
125 kDa
50 kDa
36 kDa
NC+siNC
siMYC+NC
siNC+KDM1A
siMYC+KDM1A
D
Relative protein expression level
CHOP
PERK
ATF4
NC+siNC
siMYC+NC
siNC+KDM1A
siMYC+KDM1A

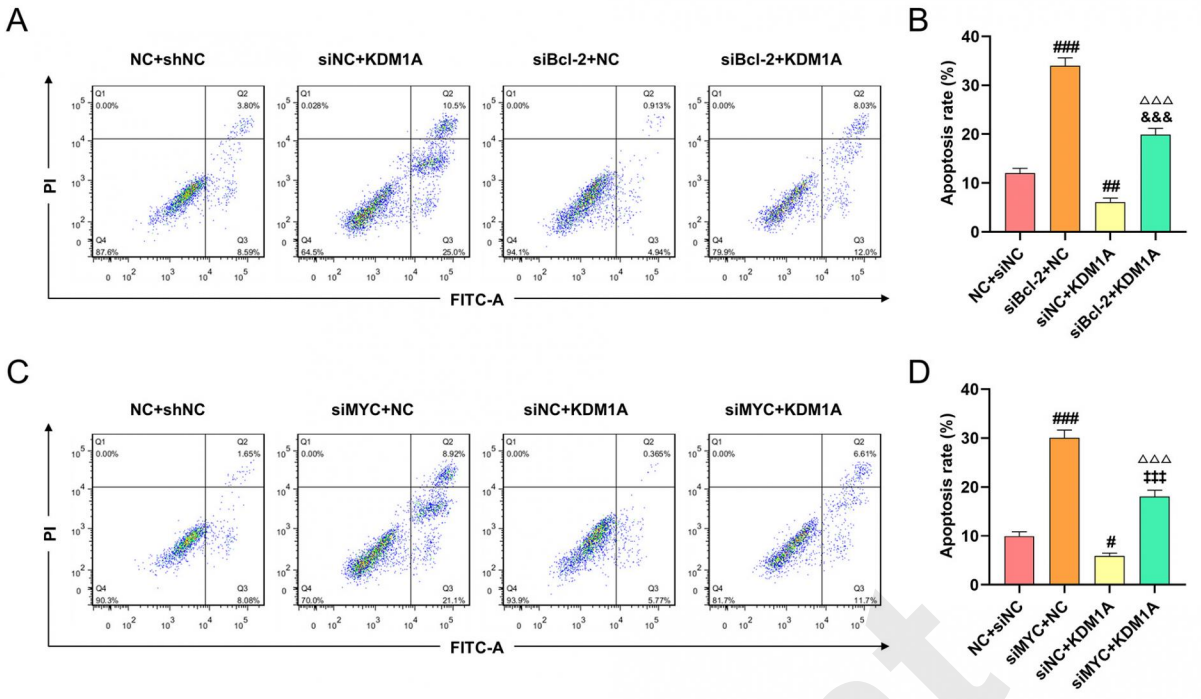
A
NC+shNC
siNC+KDM1A
siBcl-2+NC
siBcl-2+KDM1A
PI
FITC-A
B
Apoptosis rate (%)
NC+siNC
siBcl-2+NC
siNC+KDM1A
siBcl-2+KDM1A
C
NC+shNC
siMYC+NC
siNC+KDM1A
siMYC+KDM1A
PI
FITC-A
D
Apoptosis rate (%)
NC+siNC
siMYC+NC
siNC+KDM1A
siMYC+KDM1A